European Journal of Sustainable Development Research
2020, 4(3), em0126
e-ISSN: 2542-4742
https://www.ejosdr.com/

Research Article

MODESTUM
OPEN ACCESS

Slow Catalytic Pyrolysis of *Saccharum munja* using Bio-genically Synthesized Nickel Ferrite Nanoparticles for the Production of high yield Biofuel

Muhammad Imran Din [1]*, Mahnoor Javed [1], Zaib Hussain [1], Rida Khalid [1], Saba Ameen [1]

[1] Institute of Chemistry, University of Punjab, Lahore-54590, PAKISTAN
***Corresponding Author:** imrandin2007@gmail.com

Citation: Din, M. I., Javed, M., Hussain, Z., Khalid, R., & Ameen, S. (2020). Slow Catalytic Pyrolysis of *Saccharum munja* using Bio-genically Synthesized Nickel Ferrite Nanoparticles for the Production of high yield Biofuel. *European Journal of Sustainable Development Research, 4*(3), em0126. https://doi.org/10.29333/ejosdr/7900

ARTICLE INFO

Received: 29 Dec. 2019

Accepted: 31 Mar. 2020

ABSTRACT

In this study, the slow pyrolysis has been performed in a fixed bed reactor using *Saccharum munja* (munj) as raw biomass material and bio-genically synthesized nickel ferrite nanoparticles (NF-NPs) as a catalyst at an optimum temperature of 450 °C. In the absence of any catalyst, the obtained yield of bio-oil was 43.3 %. The maximum yield of bio-oil (72 %) was obtained with 0.4 g of NF-NPs. With 0.2g of ZSM-5, the obtained bio-oil yield was 44.5 %. The characterization of NF-NPs was studied by using UV-VIS analysis and Fourier Transform Infrared (FT-IR) spectroscopy. The characterization of Bio-char was done by using FT-IR spectroscopy.

Keywords: *Saccharum munja, N*ickel ferrite nanoparticles, Catalytic pyrolysis, Bio-oil, Green synthesis, Nanotechnology

INTRODUCTION

Nanoparticles are synthesized by various chemical means like co-precipitation or by green method etc. (Din et al., 2020; Kandpal et al., 2014). Nanoparticles have a vast variety of applications in different areas of medical science (Pasban Ziyarat et al., 2014), agriculture (Nair et al., 2010), water treatment (Farooqi et al., 2019), energy and transportation (Abedi et al. 2011). Green chemistry refers to the scheming of chemical products and their processes to eradicate or limit the usage and generation of harmful substances (Anastas & Eghbali 2010; Din et al., 2020). Green synthesis of metal nanoparticles mainly includes plants that possess alkaloids, phenols, terpenoids, and tannins. The plant also acts as a reducing and capping agent to convert the metal ions into the zero-valent state by reduction process to form stable metal nanoparticles (Din et al., 2019, 2020). Nanoparticles are an effective catalyst for the pyrolysis of biomass. Mostly metallic nanoparticles used are; nickel ferrite nanoparticles (NF-NPs). Nickel ferrite is used in sensors (Ahmed, 2017), microwave absorber (Che et al., 2006), nanowires and electrochromic coatings (Verma et al., 2006). The thermal breakdown of biomass in an inert environment (where oxygen is not present) in the presence of a catalyst, is known as catalytic pyrolysis. Its beginning temperature is 350-550 °C and goes towards the high temperature of about 700-800 °C (Fisher et al. ,2002). It also refers to the chemical bond's breakdown with the help of heat in a non-oxygen atmosphere. In the reaction of pyrolysis, large chains of hydrocarbons split into smaller pieces through de-polymerization, decarboxylation and aromatization reactions (Ferreira et al., 2020). The main benefit of the pyrolysis process is that it recycled waste material and gives valuable products (Scheirs & Kaminsky 2006). Pyrolysis is classified into slow (350-550 °C), flash (650-1250 °C) and fast (1050-1650 °C) pyrolysis. In a slow pyrolysis process, the time of residence of vapors are large enough (5-30 min) that the components at this state quickly combine to produce solid as well as liquid materials. High residence time also affects the quality and amount of bio-fuel obtained (Tippayawong et al., 2008). In slow pyrolysis, the major by-product obtained is biochar (Tomczyk et al., 2020). The slow pyrolysis process takes more time (up to an hour) for completion as compared to flash and fast pyrolysis. The heating rate for slow, flash and fast pyrolysis is 0.2-1.1, 10-200, and greater than 1000 K/s. Furthermore, in flash pyrolysis maximum quantity of bio-oil (75%) attained. But flash pyrolysis has one major drawback of oil rusting due to poor temperature stability. In fast pyrolysis, the biomass size should be less than 2 mm and a high heating rate along with a short period for vapor stay (Jeong et al., 2020). Various important factors affect the process of pyrolysis such as alkali metal (Oasmaa et al., 2015), the temperature of biomass used in pyrolysis, amount of, size of the particle (Zhou et al., 2014), time of residence of vapors (Zhou et al., 2013), pressure, and rate of heating (Montoya et al., 2017). With diverse biomasses, various types of catalysts are investigated (Nokkosmäki et al., 2000). ZSM-5, when used in pyrolysis reaction, helps in the refining of aromatic content but on the other hand, it reduces the yield of liquid (Zhang et al., 2013). But in the case of silica-alumina, the yield of char and gaseous products increases (Zabeti et al., 2012).

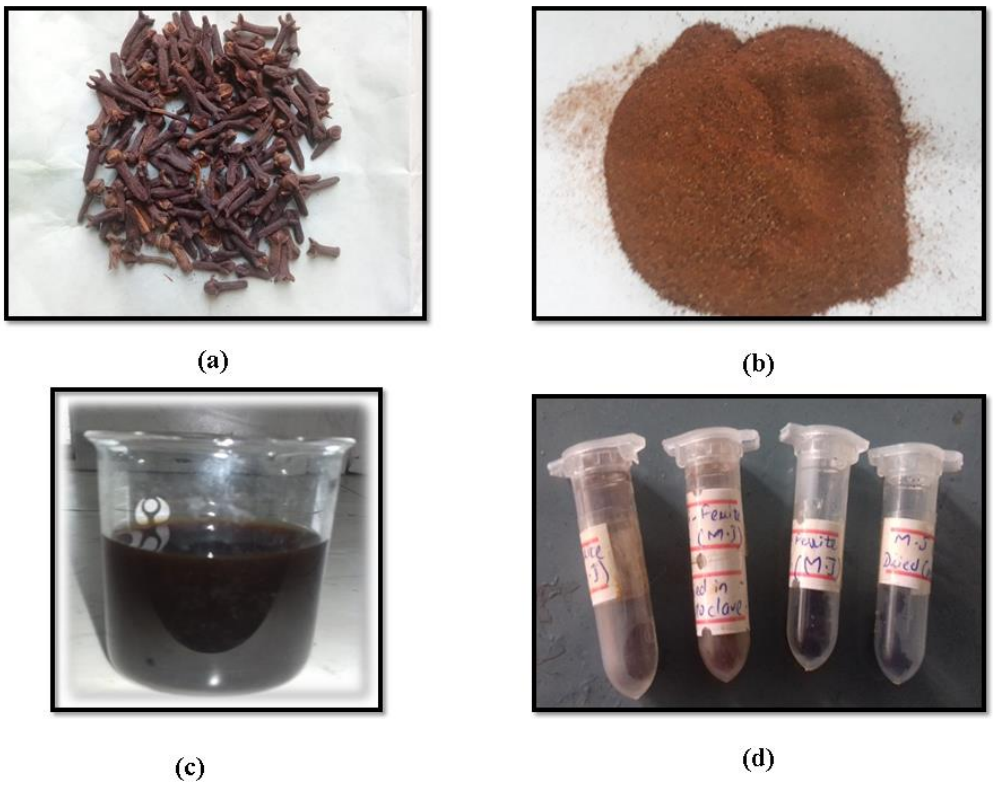

Figure 1. (a) *Syzygium aromaticum* (clove) (b) Powdered *Syzygium aromaticum (c) Syzygium aromaticum* (clove) 5% extract (d) NF-NPs

The most important catalyst used in pyrolysis includes Metal oxides or Zeolites. Metal oxides include Cu/Al_2O_3 (Chattopadhyay et al., 2009), ZnO (Zhou et al., 2013), MgO (Pütün, 2010), MnO, CaO, CuO (Chen, 2003) were used in pyrolysis reaction. In Zeolites, ZSM-5 is very common, but HZSM-5 is also used (Foster et al., 2012). Among various biomasses, *Saccharum munja* usually termed as munj belongs to the grass family and mostly found in dry areas in Pakistan. Its extract has many benefits in the area of nanotechnology, medical science, and ecology. It helps in reduction of dyspraxia and heat burns (Rahar et al., 2010). It can be used as biomass for the production of bio-products (bio-fuel and bio-char).

In line with the biogenic synthesis of NPs, to the best of our knowledge, this is a novel study on the fabrication of NF-NPs using plant extract of *Syzygium aromaticum* (clove). The plant extract contains alkaloids, flavonoids, phenols and terpenoids which have a high ability to act as reducing and capping agents. Furthermore, the catalytic efficiency of bio-genically synthesized NF-NPs is studied by the slow pyrolysis of *Saccharum munja*. A catalyst increases the efficiency and yield of pyrolysis products as well as decrease the time of reaction. *Saccharum munja* is easily available, cost-effective, and has low moisture content so it can be used as a biomass in the pyrolysis process and gives energy which is of low cost. Characterization of plant assisted synthesis of NF-NPs has been studied with UV-VIS analysis and FT-IR technique. Characterization of obtained by-products bio-oil or biochar has been done by FT-IR.

EXPERIMENTAL

Materials

Nickel nitrate hexahydrate ($Ni(NO_3)_2.6H_2O$) (~97%) and Iron nitrate nonahydrate ($Fe(NO_3)_3.9H_2O$) (≥98%) were bought from Sigma-Aldrich. These chemicals were of analytical grade hence they need no additional purification. *Syzygium aromaticum* (clove) was taken from the local market, Lahore, Pakistan. The *Saccharum munja* was collected as biomass feedstock from the city of Lahore in Punjab Province Pakistan. Prior to all the procedures the biomass was air-dried, grounded in a rotary cutting mil with a 2-6 mm particle size and then dried at 60 ^{O}C until constant weight attained.

Preparation of Plant Extract

Syzygium aromaticum (clove) was washed with distilled water for removal of impurities as shown in **Figure 1a**. Then it was dried in an oven for 2 hr for the removal of moisture and ground into a fine powder (**Figure 1b**). For the preparation of 5% extract, 5 g of clove powder was dissolved in 100 mL of de-ionized water. Then, it was placed on a hot plate at 70-80 ^{O}C for 15-20 min with constant magnetic stirring. The solution was then filtered by using Whatman's filter paper. The filtrate was stored at 40 ^{O}C in the refrigerator for further use (**Figure 1c**). Phytochemical analysis of clove extract was performed which shows that it can act as strong reducing as well as capping agent.

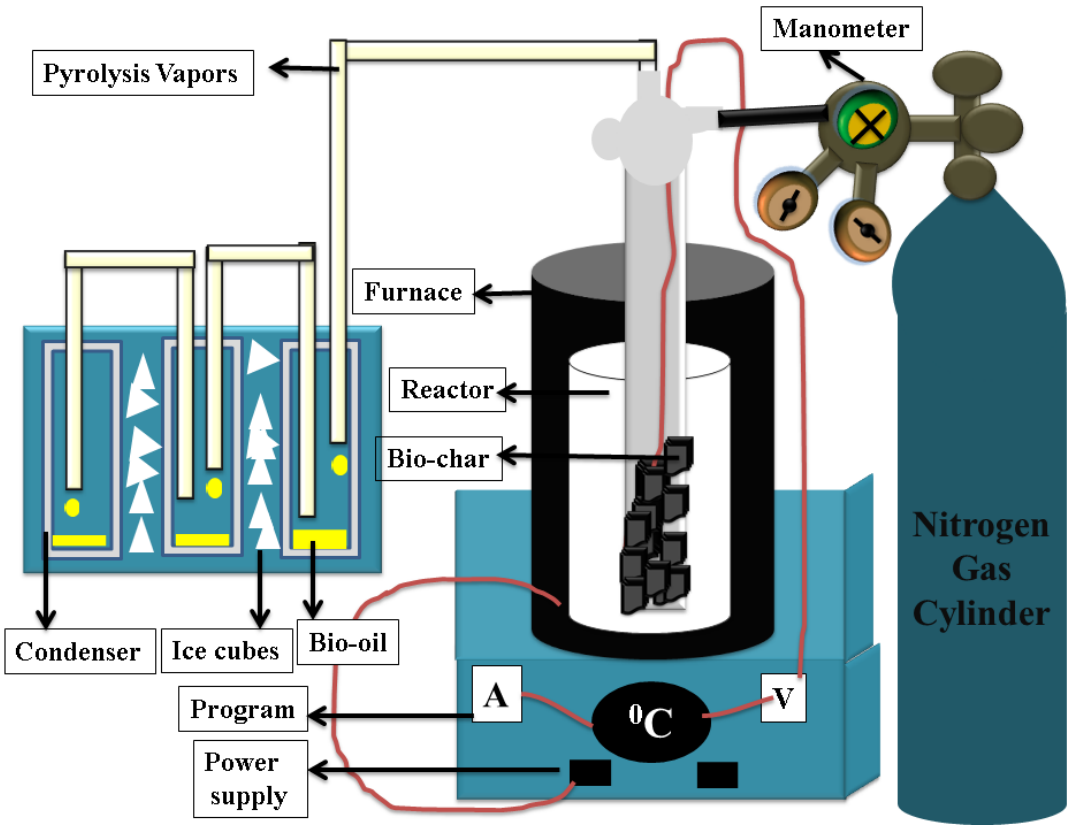

Figure 2. Schematic diagram of reactor used for pyrolysis of *Saccharum munja* biomass feedstock

Synthesis of Ni-Fe_2O_4 Nanoparticles

Nanoparticles were prepared by microwave combustion method (MCM). For this purpose, 10 mL of 2% [$Ni(NO_3)_2.6H_2O$] and 10 ml of 8% [$Fe(NO_3)_3.9H_2O$] were added in 100 ml beaker. Then, they were stirred together for 1 hr. Then, 20 ml of *Syzygium aromaticum* (clove) extract was added in it and again stirred together for 30 min. The obtained solution was then poured in an autoclave and subjected to a microwave oven for 10 min. After that, the autoclave was placed in an oven at 200 ^{O}C for 24 hr. At last, the solution from autoclave was poured into a petri dish. 1 mL was taken for the UV-VIS analysis. The remaining solution was dried in an oven at 65 ^{O}C for 1-2 days. NF-NPs were prepared and stored in airtight sample bottles as shown in **Figure 1d**.

Pyrolysis Procedure

The process of pyrolysis was performed in a reactor which was made up of stainless steel and the type of reactor is a fixed-bed reactor as shown in **Figure 2**. In this process, 10 g of biomass (*Saccharum munja)* was taken in a pyrolysis reactor tube. After that, the inert gas nitrogen supply with a flow rate of 150 mL/min was provided in order to ensure oxygen-free environment. All the apparatus was tightly sealed by using Plaster of Paris or by a special type of tape. The output pipes had a connection with the sample gathering bottles as well as with the pyrolysis tube. The bottles were placed in chromatographic tanks having a certain amount of ice in them. Ice was used to lower the temperature and condense the vapors into liquid. In the first chromatographic tank, NaCl is added which allows the gathering of all the bio-oil in 1st sample bottle. The heat supply was provided by setting the temperature of the pyrolysis reactor at 450 ^{O}C. Temperature raised at the rate of 10 ^{o}C/min. Hence, optimum conditions were provided to achieve maximum yield of pyrolysis by-products. The reaction was completed within 45-50 min. Bio-oil was collected from bottles and stored in sample bottles while bio-char was collected from the pyrolysis tube and kept in airtight packets. The same method was repeated with 0.2, 0.3, and 0.4 g of NF-NPs were added as a catalyst along with 10 g of *Saccharum munja*. Another experiment with 0.2 g of ZSM-5 catalyst was added along with 10 g of *Saccharum munja* (munj) in the reactor tube. Additionally, the percentage yield of products obtained can be calculated by applying formula;

$$\text{Yield of Bio} - \text{oil } (\%) = \frac{\text{Weight of Bio oil}}{\text{Initial weight of Bio mass}} \times 100$$

$$\text{Yield of Biochar } (\%) = \frac{\text{Weight of Bio char}}{\text{Initial weight of Bio mass}} \times 100$$

$$\text{Yield of Bio} - \text{gas } (\%) = 100 - (\text{Yield of Bio} - \text{oil} + \text{Yield of BioChar})$$

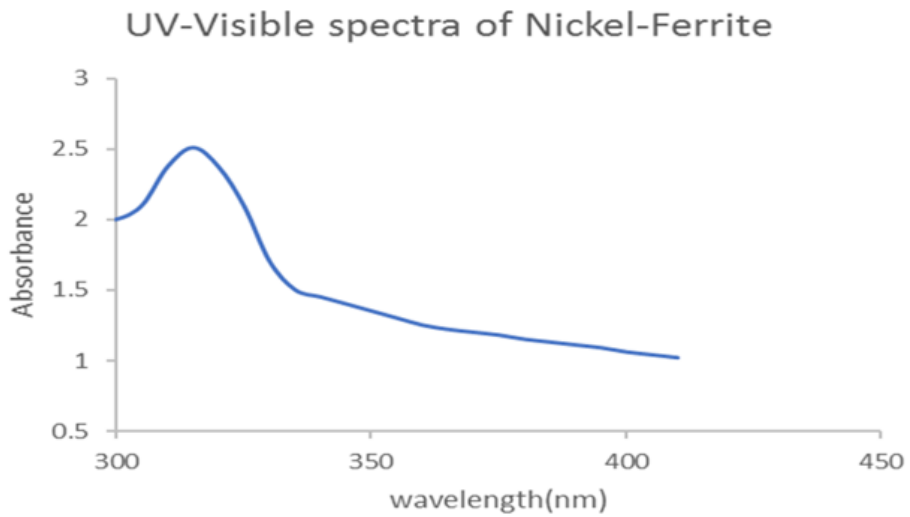

Figure 3. Absorbance spectra of NF-NPs

Characterization

The Nickel ferrite (Ni-Fe_2O_4) nanoparticles prepared by the green method were characterized for their optical properties by using UV-VIS spectrophotometer (UVD-3500, Labomed Inc. USA Double beam and resolution of 0.1 nm). Ultraviolet-visible spectroscopy is a useful technique for the analysis of nanoparticle. It is the first step for the conformation of nanoparticles formation by analyzing the maximum peak of absorption and estimating conduction band oscillations in response to the electromagnetic radiations. UV-VIS analysis gives the results in the range of 200-800 nm. The Perkin Elmer, RX 1 FT-IR spectrophotometer was employed to scan the FT-IR pattern of nanoparticles as well as of bio-char. For this purpose prepared nanoparticles and biochar were separately taken in a sample bottle and then the spectrum was attained from 4000 to 650 cm^{-1} (near infra-red region) for defining structural moieties of biochar and nanoparticles (Maensiri et al., 2007).

RESULTS AND DISCUSSION

UV-VIS Analysis of Nickel-Ferrite Nanoparticles

The production of NF-NPs by reducing metallic ions in the MCM method was verified by the UV-VIS spectroscopy. All the metallic nanoparticles have a specific color change which is depending upon their respective shape and size. The appearance of NF-NPs changed from black to reddish-brown. It has been observed that the characteristic band for NF-NPs developed in the range 300-420 nm due to the dispersion and absorption phenomenon of magnetic NF-NPs and it is in complete agreement with previous studies (Rodrigues et al., 2015). Here, NF-NPs provide a maximum absorption peak at 310 nm displayed in **Figure 3**. Stability, large yield and well-dispersity of nanoparticles are confirmed by the sharpness as well the intensity of the peak. No additional peak represents the purity of NF-NPs.

FT-IR Characterization of Nickel Ferrite NPs

For the identification of different functional groups in NF-NPs, FT-IR analysis was done as shown in **Figure 4**. Usually, metal oxides form absorption peaks in the fingerprint region normally less than 1000 cm^{-1}. These absorption bands are due to vibrations among different atomic levels. The peak formed at 3352.94 cm^{-1} is due to the symmetric vibration of a hydroxyl group. Meanwhile, the absorption band at 1038 cm^{-1} shows the bending vibrations of -OH group. A peak at 1573.97 cm^{-1} corresponds to the presence of C=C symmetric stretching. The peaks at 2889 and 1357 cm^{-1} are for stretching vibration of CH_2. The absorption peaks at 597 cm^{-1} and 508.13 cm^{-1} represent the M-O in the nickel ferrite (Mohammed et al., 2020). Additionally, these two peaks represent the tetrahedral and octahedral structure of the positive ion of nickel ferrite (Kamnev & Ristić, 1997). Stretching of the CH_3 group is shown by peak at 2851 cm^{-1}. The absorption bands of NF-NPs are correlated with the values given in the literature reported by Sivakumar et al. (2011). **Figures 5** and **6** showed the FT-IR analysis of bio-char of *Saccharum munja* in the absence and presence of a catalyst. The visible band at 746, 1037, 1118, 1446, 1556, 2163 and 3146 cm^{-1} indicates the present content of organic residues i.e. C-C aromatic bending in fatty acid, lignin and polysaccharides, hydroxyl group and polymeric CH_3 group, respectively. A band at 747 cm^{-1} indicates C-H aromatic bending which indicates the presence of aromatic in synthesized biochar. Absorption bands at 1038 and 1446 cm^{-1} represent the C-O stretching vibrations which correspond to the presence of ketones, alcohol, phenols, and esters. The absorbance peak at 1556 cm^{-1} shows the possibility of stretching vibration of the C=C group due to the presence of lignin. Similar results have been reported by Kumar et al. (2017). C=C bending vibration is indicated by 2165 cm^{-1}.

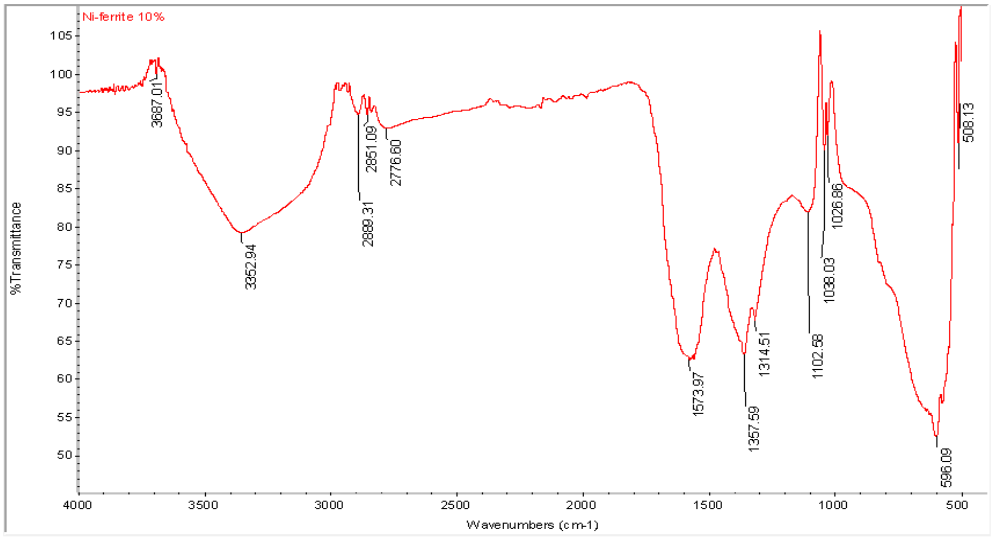

Figure 4. FT-IR spectrum of NF-NPs

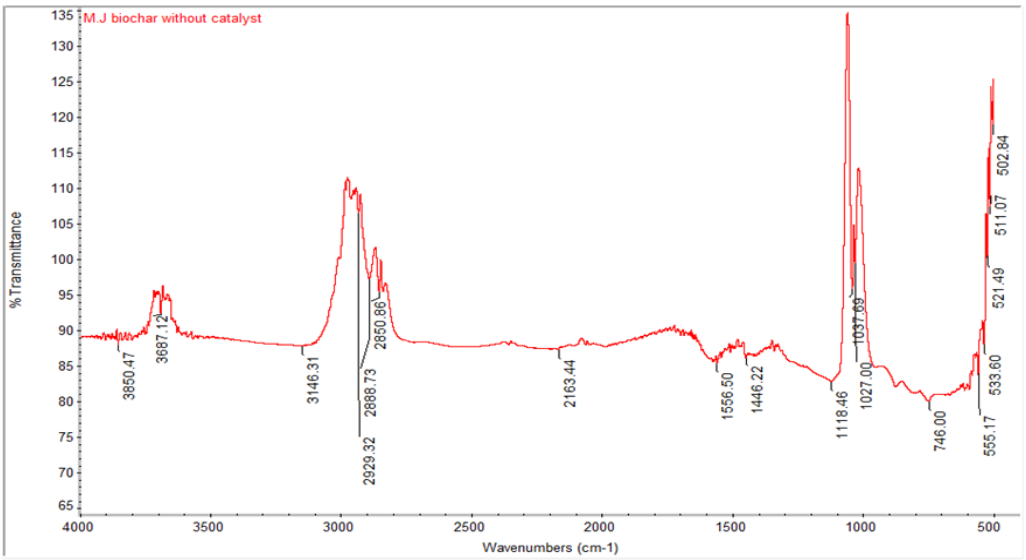

Figure 5. FT-IR spectrum of Bio-char without Catalyst

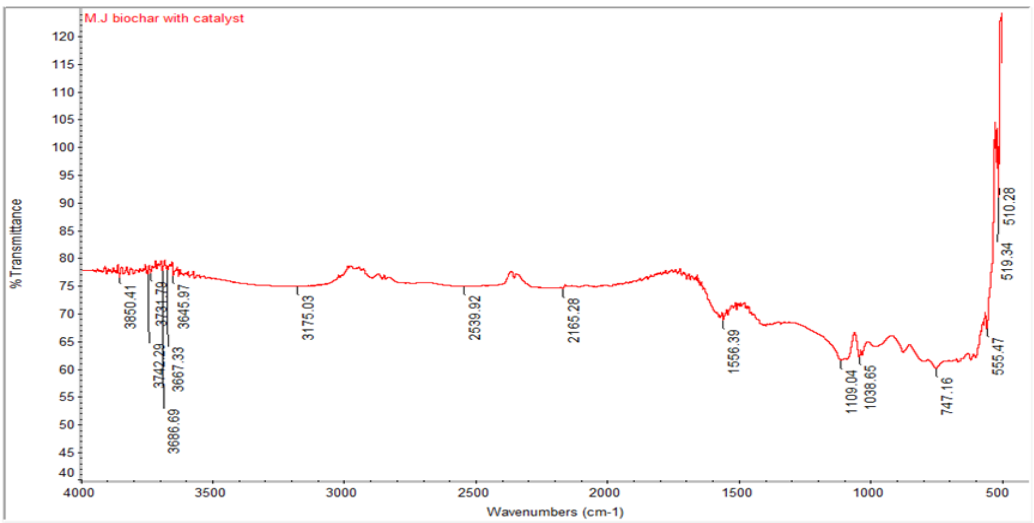

Figure 6. FT-IR spectrum of Bio-char with Catalyst

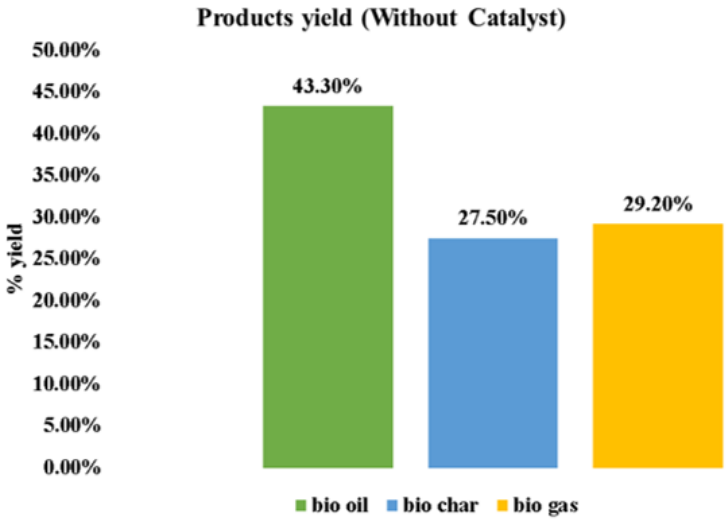

Figure 7. Slow Catalytic pyrolysis of *Saccharum munja* without Catalyst

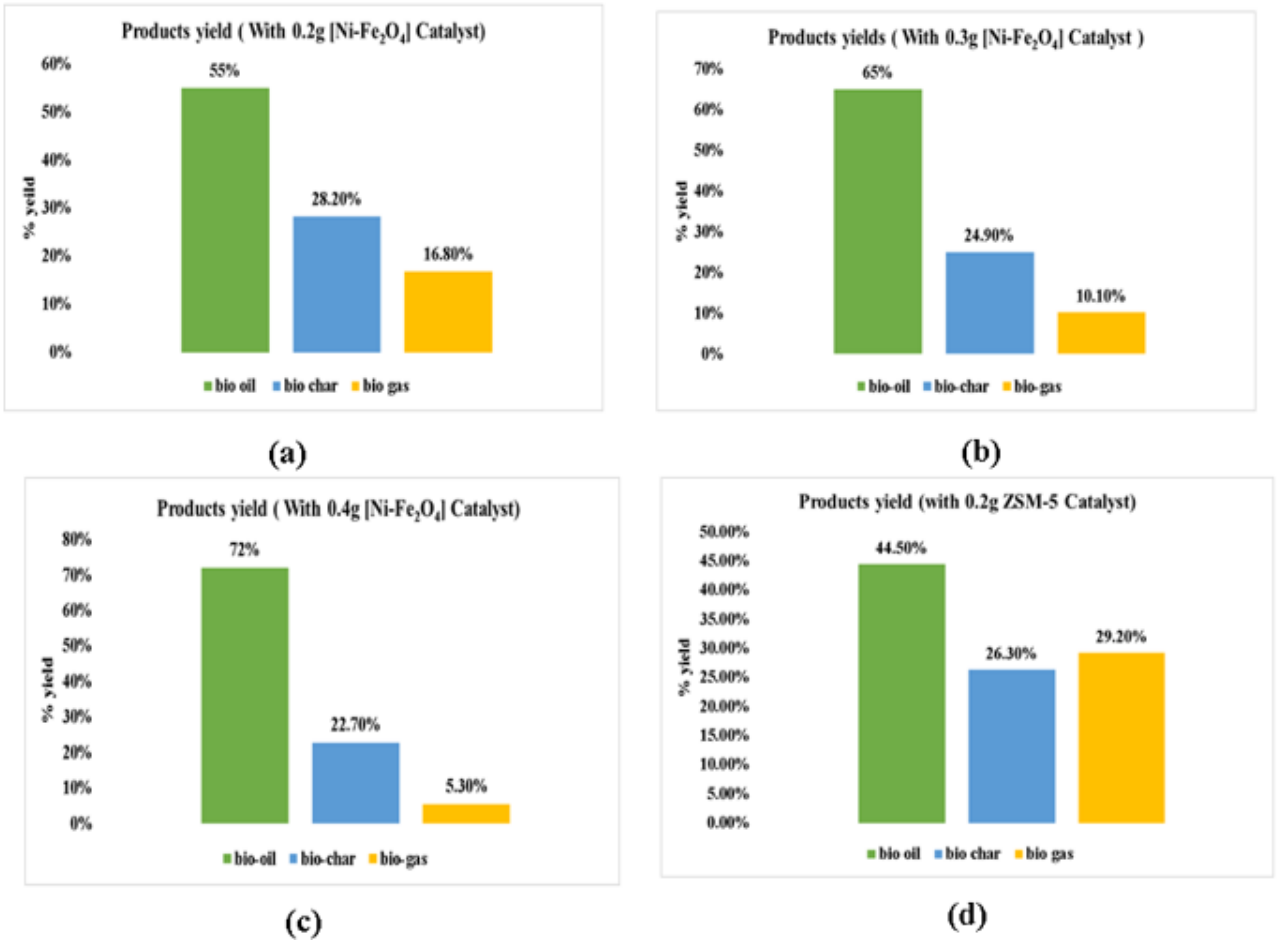

Figure 8. Slow Catalytic Pyrolysis of *Saccharum munja* (a) 0.2g NF-NPs (b) 0.3g NF-NPs (c) 0.4g NF-NPs (d) 0.2 g ZSM-5

Percentage Yields of Pyrolytic Products

Figure 7 displayed the slow Pyrolysis of *Saccharum munja* without a catalyst. In the absence catalyst, the by-products obtained at 450 ^{O}C are bio-oil (43.3%), bio-char (27.5%) and bio-gas (29.2%). While by-products obtained in the presence of 0.2g NF-NPs are bio-oil (55%), bio-char (28.2%) and bio-gas (16.8%) as shown in **Figure 8a**. Slow catalytic pyrolysis of *Saccharum munja* with 0.3g NF-NPs gave bio-oil (65%), bio-char (24.90%) and bio-gas (10.10%) at 450 ^{O}C (**Figure 8b**). By pyrolysis of *Saccharum munja*, the by-products obtained which is bio-oil (72%), bio-char (22.70%) and bio-gas (5.30%) at 450 ^{O}C by using 0.4g of NF-NPs (**Figure 8c**). Additionally, in the presence of 0.2g of ZSM-5 the by-products were obtained are bio-oil (44.5%), bio-char (26.3%) and bio-gas (29.2%) at 450 ^{O}C (**Figure 8d**).

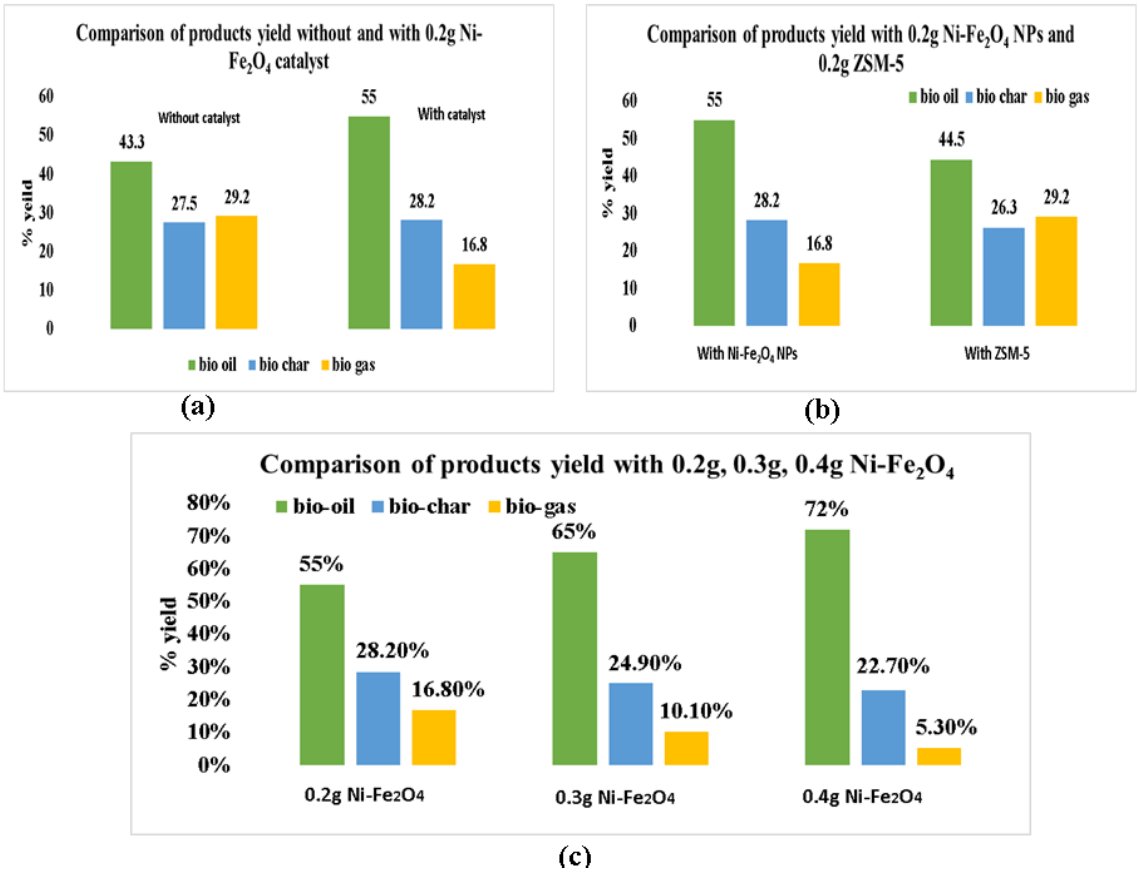

Figure 9. Comparison of Products yields (a) without catalyst and with 0.2g NF-NPs (b) 0.2g NF-NPs and 0.2g ZSM-5 (c) 0.2g, 0.3g and 0.4g NF-NPs

A comparison of yields in the presence of various catalysts provides feasibility to find a better catalyst. **Figure 9a** showed that there was a considerable increase in yield of bio-oil and bio-char in presence of [$Ni\text{-}Fe_2O_4$] nanoparticles. This proved that nickel ferrite nanoparticles were an efficient catalyst for the pyrolysis of biomass. Meanwhile, **Figure 9b** shows a comparison of NF-NPs and ZSM-5 in the process of pyrolysis of *Saccharum munja*. It is confirmed from the figure that by using NF-NPs as catalyst high yield of bio-oil (55%) was obtained while with ZSM-5 (44.5%) bio-oil was obtained. Comparison of yields of bio-oil, bio-char and bio-gas by using 0.2g, 0.3g, 0.4g $Ni\text{-}Fe_2O_4$ NPs (catalyst) has been displayed in **Figure 9c**. It had been shown from the graph that, by an increase in the amount of the catalyst, the yield of bio-oil was increased. The bio-oil yield was increased from 55% to 65% and then to 72%. The increase in yield confirms that NF-NPs act as a highly efficient catalyst in the pyrolysis of *Saccharum munja*. The catalyst mainly increases the speed of reaction. Hence, in pyrolysis of *Sacchrum munja* without catalyst, the yield is low so ZSM-5 as a catalyst was used to increase the yield of bio-oil but the yield was only increased by 1-2%. Then another catalyst Nickel-Ferrite NPs was used in different amount which increased the yield of bio-oil very effectively. This concludes that nickel ferrite NPs acted as a more efficient catalyst than ZSM-5 for enhancing the yield of bio-oil.

According to the experimental reports and pervious literature, the chemical reaction pyrolysis action of nanoparticles was suggested.

$$\text{Biomass} \rightarrow \text{Cellulose} + \text{Lignin} + \text{Hemicellulose} \quad (1)$$

$$\text{Cellulose} \rightarrow \text{Anhydrosugar} \rightarrow \text{Furan} \rightarrow \text{Hydrocabon pool} \rightarrow \text{Aromatic Hydrocarbon} \rightarrow \text{Coke} \quad (2)$$

$$\text{Hemicellulose} \rightarrow \text{Furan} + \text{Pyrans} \rightarrow \text{Hydrocabon pool} \rightarrow \text{Aromatic Hydrocarbon} \rightarrow \text{Coke} \quad (3)$$

$$\text{Lignin} \rightarrow \text{Phenols} \rightarrow \text{Coke} \quad (4)$$

Equation 1-4 showed that during catalytic pyrolysis the biomass component cellulose depolymerized into anhydrosugars (Zheng et al., 2019). The anhydrosugars after dehydration, decarboxylation, and decarbonylation converted into furans which diffuse into channels of NF-NPs catalyst undergo oligomerization to form hydrocarbon pool and coke product obtained. Lignin and hemicellulose after thermal breakdown depolymerized into phenol, pyrans, and furans respectively. The phenol, pyrans or furans diffuse into pores of NF-NPs catalyst which after dehydration or condensation converted into coke.

CONCLUSION

Biogenically synthesized highly efficient NF-NPs were used for the efficient conversion of biomass thermo-chemically. *Saccharum munja* (munj) possesses excellent characteristics to be used as biomass in slow catalytic pyrolysis for the production of bioenergy. As a waste, munj is highly cost-effective for the production of bio-oil, bio-char, and bio-gas, as well as it comprises less dangerous effects on the environment. Pyrolysis of *Saccharum munja* was carried out without any catalyst which gives a yield of by-products as bio-oil (43.3%), bio-char (27.50%) and bio-gas (29.20%). The same reaction was performed with 0.2g of NF-NPs as a catalyst, which gives bio-oil (55%), bio-char (28.20%) and bio-gas (16.80%). With 0.3g catalyst (65%) bio-oil, (24.90%) bio-char and (10.10%) bio-gas was obtained. With 0.4g catalyst (72%) bio-oil was obtained. The amount of catalyst has a considerable effect on bio-oil yield. It increases from 43.3% to 55% then 65% and finally to 72%. All the reactions were carried out at 450 ^{O}C . An additional reaction was carried out with 0.2g ZSM-5 which gives (44.5%) bio-oil yield. It shows that NF-NPs are more efficient catalyst than ZSM-5 for pyrolysis of *Saccharum munja*. The maximum yield of bio-oil (72%) was obtained with a 0.4g catalyst. FT-IR characterization of bio-char was performed for the analysis of the functional group.

REFERENCES

Abedi, G., Sotoudeh, A., Soleymani, M., Shafiee, A., Mortazavi, P., & Aflatoonian, M.R. (2011). A collagen–poly (vinyl alcohol) nanofiber scaffold for cartilage repair. Journal of Biomaterials Science, Polymer Edition, 22(18), 2445-2455 https://doi.org/10.1163/092050610X540503

Ahmed, M. A. A. (2017). *A review on the properties and uses of ferrite magnet*. Sudan University of Science and Technology. Retrieved from http://repository.sustech.edu/handle/123456789/19434

Anastas, P., & Eghbali, N. (2010). Green chemistry: Principles and practice. *Chemical Society Reviews, 39*(1), 301-312. https://doi.org/10.1039/B918763B

Chattopadhyay, J., Kim, C., Kim, R., & Pak, D. (2009). Thermogravimetric study on pyrolysis of biomass with Cu/Al2O3 catalysts. *Journal of Industrial and Engineering Chemistry, 15*(1), 72-76. https://doi.org/10.1016/j.jiec.2008.08.022

Che, R., Zhi, C., Liang, C., & Zhou, X. (2006). Fabrication and microwave absorption of carbon nanotubes / CoFe2O4 spinel nanocomposite. *Applied Physics Letters, 88*(3), 033105. https://doi.org/10.1063/1.2165276

Chen, G. (2003). Catalytic application to biomass pyrolysis in a fixed bed reactor. *Energy sources, 25*(3), 223-228. https://doi.org/10.1080/00908310390142271

Din, M. I., Khalid, R., & Hussain, Z. (2020). Recent research on development and modification of nontoxic semiconductor for environmental application. *Separation & Purification Reviews*, 1-18. https://doi.org/10.1080/15422119.2020.1714658

Din, M. I., Najeeb, J., Hussain, Z., Khalid, R., & Ahmad, G. (2020). Biogenic scale up synthesis of ZnO nano-flowers with superior nano-photocatalytic performance. *Inorganic and Nano-Metal Chemistry*, 1-7. https://doi.org/10.1080/24701556.2020.1723026

Din, M. I., Rani, A., Hussain, Z., Khalid, R., Aihetasham, A., & Mukhtar, M. (2019). Biofabrication of size-controlled ZnO nanoparticles using various capping agents and their cytotoxic and antitermite activity. *International Journal of Environmental Analytical Chemistry*, 1-17. https://doi.org/10.1080/03067319.2019.1672671

Din, M. I., Tariq, M., Hussain, Z., & Khalid, R. (2020). Single step green synthesis of nickel and nickel oxide nanoparticles from hordeum vulgare for photocatalytic degradation of methylene blue dye. *Inorganic and Nano-Metal Chemistry*, 1-6. https://doi.org/10.1080/24701556.2019.1711401

Farooqi, Z. H., Khalid, R., Begum, R., Farooq, U., Wu, Q., Wu, W., … Naseem, K. (2019). Facile synthesis of silver nanoparticles in a crosslinked polymeric system by in situ reduction method for catalytic reduction of 4-nitroaniline. *Environmental technology, 40*(15), 2027-2036. https://doi.org/10.1080/09593330.2018.1435737

Ferreira, A. F., Ferreira, A., Dias, A. P. S., & Gouveia, L. (2020). Pyrolysis of scenedesmus obliquus biomass following the treatment of different wastewaters. *BioEnergy Research*, 1-11. https://doi.org/10.1007/s12155-020-10102-1

Fisher, T., Hajaligol, M., Waymack, B., & Kellogg, D. (2002). Pyrolysis behavior and kinetics of biomass derived materials. *Journal of analytical and applied pyrolysis, 62*(2), 331-349. https://doi.org/10.1016/S0165-2370(01)00129-2

Foster, A. J., Jae, J., Cheng, Y.-T., Huber, G. W., & Lobo, R. F. (2012). Optimizing the aromatic yield and distribution from catalytic fast pyrolysis of biomass over zsm-5. *Applied Catalysis A: General, 423*, 154-161. https://doi.org/10.1016/j.apcata.2012.02.030

Jeong, J.-Y., Yang, C.-W., Lee, U.-D., & Jeong, S.-H. (2020). Characteristics of the pyrolytic products from the fast pyrolysis of palm kernel cake in a bench-scale fluidized bed reactor. *Journal of Analytical and Applied Pyrolysis, 145*, 104708. https://doi.org/10.1016/j.jaap.2019.104708

Kamnev, A. A., & Ristić, M. (1997). Fourier transform far-infrared spectroscopic evidence for the formation of a nickel ferrite precursor in binary Ni (II)-Fe (III) hydroxides on coprecipitation. *Journal of molecular structure, 408*, 301-304. https://doi.org/10.1016/S0022-2860(96)09485-9

Kandpal, N., Sah, N., Loshali, R., Joshi, R., & Prasad, J. (2014). *Co-precipitation method of synthesis and characterization of iron oxide nanoparticles*.

Kumar, P., Kumar, P., Rao, P. V., Choudary, N. V., & Sriganesh, G. (2017). Saw dust pyrolysis: Effect of temperature and catalysts. *Fuel, 199*, 339-345. https://doi.org/10.1016/j.fuel.2017.02.099

Maensiri, S., Masingboon, C., Boonchom, B., & Seraphin, S. (2007). A simple route to synthesize nickel ferrite (NiFe2O4) nanoparticles using egg white. *Scripta materialia, 56*(9), 797-800. https://doi.org/10.1016/j.scriptamat.2006.09.033

Mohammed, F. A., Khalaf, M. M., Mohamed, I. M., Saleh, M., & Abd El-Lateef, H. M. (2020). Synthesis of mesoporous nickel ferrite nanoparticles by use of citrate framework methodology and application for electrooxidation of glucose in alkaline media. *Microchemical Journal, 153*, 104507. https://doi.org/10.1016/j.microc.2019.104507

Montoya, J., Pecha, B., Roman, D., Janna, F. C., & Garcia-Perez, M. (2017). Effect of temperature and heating rate on product distribution from the pyrolysis of sugarcane bagasse in a hot plate reactor. *Journal of analytical and applied pyrolysis, 123*, 347-363. https://doi.org/10.1016/j.jaap.2016.11.008

Nair, R., Varghese, S. H., Nair, B. G., Maekawa, T., Yoshida, Y., & Kumar, D. S. (2010). Nanoparticulate material delivery to plants. *Plant science, 179*(3), 154-163. https://doi.org/10.1016/j.plantsci.2010.04.012

Nokkosmäki, M., Kuoppala, E., Leppämäki, E., & Krause, A. (2000). Catalytic conversion of biomass pyrolysis vapours with zinc oxide. *Journal of Analytical and Applied Pyrolysis, 55*(1), 119-131. https://doi.org/10.1016/S0165-2370(99)00071-6

Oasmaa, A., Sundqvist, T., Kuoppala, E., Garcia-Perez, M., Solantausta, Y., Lindfors, C., & Paasikallio, V. (2015). Controlling the phase stability of biomass fast pyrolysis bio-oils. *Energy & Fuels, 29*(7), 4373-4381. https://doi.org/10.1021/acs.energyfuels.5b00607

Pasban Ziyarat, F., Asoodeh, A., Sharif Barfeh, Z., Pirouzi, M., & Chamani, J. (2014). Probing the interaction of lysozyme with ciprofloxacin in the presence of different-sized ag nano-particles by multispectroscopic techniques and isothermal titration calorimetry. *Journal of Biomolecular Structure and Dynamics, 32*(4), 613-629. https://doi.org/10.1080/07391102.2013.785919

Pütün, E. (2010). Catalytic pyrolysis of biomass: Effects of pyrolysis temperature, sweeping gas flow rate and MgO catalyst. *Energy, 35*(7), 2761-2766. https://doi.org/10.1016/j.energy.2010.02.024

Rahar, S., Nagpal, N., Swami, G., Arora, M., Bansal, S., Goyal, S., … Kapoor, R. (2010). Medicinal aspects of saccharum munja. *Research Journal of Pharmacy and Technology, 3*(3), 636-639.

Rodrigues, A. R. O., Gomes, I. T., Almeida, B. G., Araújo, J. P., Castanheira, E. M., & Coutinho, P. J. (2015). Magnetic liposomes based on nickel ferrite nanoparticles for biomedical applications. *Physical Chemistry Chemical Physics, 17*(27), 18011-18021

Scheirs, J., & Kaminsky, W. (2006). *Feedstock recycling and pyrolysis of waste plastics*. UK : John Wiley & Sons Chichester.

Sivakumar, P., Ramesh, R., Ramanand, A., Ponnusamy, S., & Muthamizhchelvan, C. (2011). Synthesis and characterization of nickel ferrite magnetic nanoparticles. *Materials Research Bulletin, 46*(12), 2208-2211. https://doi.org/10.1016/j.materresbull.2011.09.009

Tippayawong, N., Kinorn, J., & Thavornun, S. (2008). Yields and gaseous composition from slow pyrolysis of refuse-derived fuels. *Energy Sources, Part A, 30*(17), 1572-1580. https://doi.org/10.1080/15567030701258550

Tomczyk, A., Sokołowska, Z., & Boguta, P. (2020). Biochar physicochemical properties: Pyrolysis temperature and feedstock kind effects. *Reviews in Environmental Science and Bio/Technology*, 1-25. https://doi.org/10.1007/s11157-020-09523-3

Verma, A., Alam, M., Chatterjee, R., Goel, T., & Mendiratta, R. (2006). Development of a new soft ferrite core for power applications. *Journal of Magnetism and Magnetic Materials, 300*(2), 500-505. https://doi.org/10.1016/j.jmmm.2005.05.040

Zabeti, M., Nguyen, T., Lefferts, L., Heeres, H., & Seshan, K. (2012). In situ catalytic pyrolysis of lignocellulose using alkali-modified amorphous silica alumina. *Bioresource technology, 118*, 374-381. https://doi.org/10.1016/j.biortech.2012.05.034

Zhang, H., Xiao, R., Jin, B., Shen, D., Chen, R., & Xiao, G. (2013). Catalytic fast pyrolysis of straw biomass in an internally interconnected fluidized bed to produce aromatics and olefins: Effect of different catalysts. *Bioresource technology, 137*, 82-87. https://doi.org/10.1016/j.biortech.2013.03.031

Zheng, Y., Tao, L., Yang, X., Huang, Y., Liu, C., & Zheng, Z. (2019). Comparative study on pyrolysis and catalytic pyrolysis upgrading of biomass model compounds: Thermochemical behaviors, kinetics, and aromatic hydrocarbon formation. *Journal of the Energy Institute, 92*(5), 1348-1363. https://doi.org/10.1016/j.joei.2018.09.006

Zhou, L., Yang, H., Wu, H., Wang, M., & Cheng, D. (2013). Catalytic pyrolysis of rice husk by mixing with zinc oxide: Characterization of bio-oil and its rheological behavior. *Fuel processing technology, 106*, 385-391. https://doi.org/10.1016/j.fuproc.2012.09.003

Zhou, S., Garcia-Perez, M., Pecha, B., McDonald, A. G., Kersten, S. R., & Westerhof, R. J. (2013). Secondary vapor phase reactions of lignin-derived oligomers obtained by fast pyrolysis of pine wood. *Energy & fuels, 27*(3), 1428-1438. https://doi.org/10.1021/ef3019832

Zhou, S., Garcia-Perez, M., Pecha, B., McDonald, A. G., & Westerhof, R. J. (2014). Effect of particle size on the composition of lignin derived oligomers obtained by fast pyrolysis of beech wood. *Fuel, 125*, 15-19. https://doi.org/10.1016/j.fuel.2014.01.016